Supplementary Information

A convenient fluorescent nanoplatform relying on N,B-doped carbon dots to achieve highly selective sensing of dichromate

Chunxiao Cui, Linlin Wang* and Xue-Bo Yin*

Institute for Frontier Medical Technology, College of Chemistry and Chemical Engineering, Shanghai University of Engineering Science, Shanghai 201620, China

*E-mail: wanglinlin@sues.edu.cn; xbyin@nankai.edu.cn

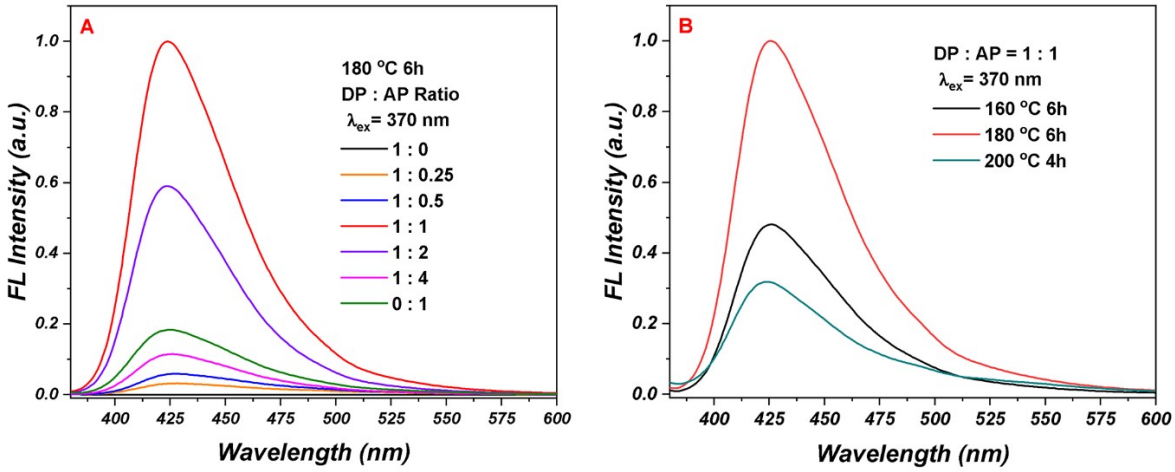

Figure S1. (A)The precursor ratios, and (B) the reaction temperature and time were optimized to observe the highest fluorescence for APDP-CDs. [obtained-CDs] = 0.039 mg/mL, λ_{ex} = 370 nm.

Calculation of the quantum yields

The fluorescence quantum yields (QYs) of the obtained APDP-CDs were determined by a relative method according to previous reports using quinine sulfate (QS) in 0.1 M H_2SO_4 (Φ_r = 54%) as the reference [27, 29]. The QYs value of the sample was calculated using the following equation:

$$\Phi_s = \Phi_r \cdot \left(I_s/A_s\right) \cdot \left(A_r/I_r\right) \cdot \left(\eta_s/\eta_r\right)^2$$
$$= \Phi_r \cdot \left(K_s \,/\, K_r\right) \cdot \left(\eta_s \,/\, \eta_r\right)^2 \quad \text{(S1)}$$

Where Φ is the relative quantum yields and η is the refractive index of the solvent. K is the slope determined by the curves. The subscript "r" refers to the reference, quinine sulfate dye dissolved in 0.1M H_2SO_4 with quantum yields (54%), and "s" for the sample. For the aqueous solutions, the refractive index $\eta_s = \eta_r = 1.33$. To get more reliable results, the optical density of the sample was kept value were between 0 – 0.06 to minimize the inner-filter effects at the excitation wavelength. The fluorescence spectra were recorded and then integrated of intensity. Figure S4 (Supplementary Information) summarizes the QYs of quinine sulfate and the obtained APDP-CDs, respectively.

	Quinine sulfate (QS)					**APDP-CDs**				
Abs.	0.010	0.020	0.031	0.041	0.050	0.010	0.021	0.030	0.040	0.051
Integrated fluorescence	1467 74.11	2251 16.41	2821 55.18	3507 94.57	4199 83.88	5194 2.35	1074 21.56	1520 15.24	1985 50.73	24010 9.62
Slope	**6643162**					**4624121**				
QYs (%)	**54**					**37.59**				

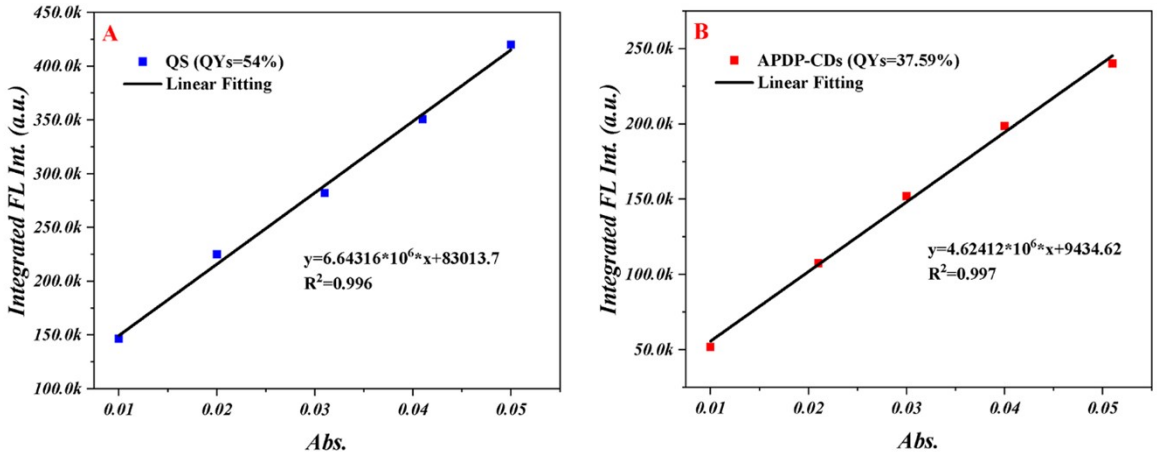

Figure S2. Plots integrated fluorescence intensity of quinine sulfate (QS, the reference) and APDP-CDs as a function of optical absorbance at 360 nm and relevant data.

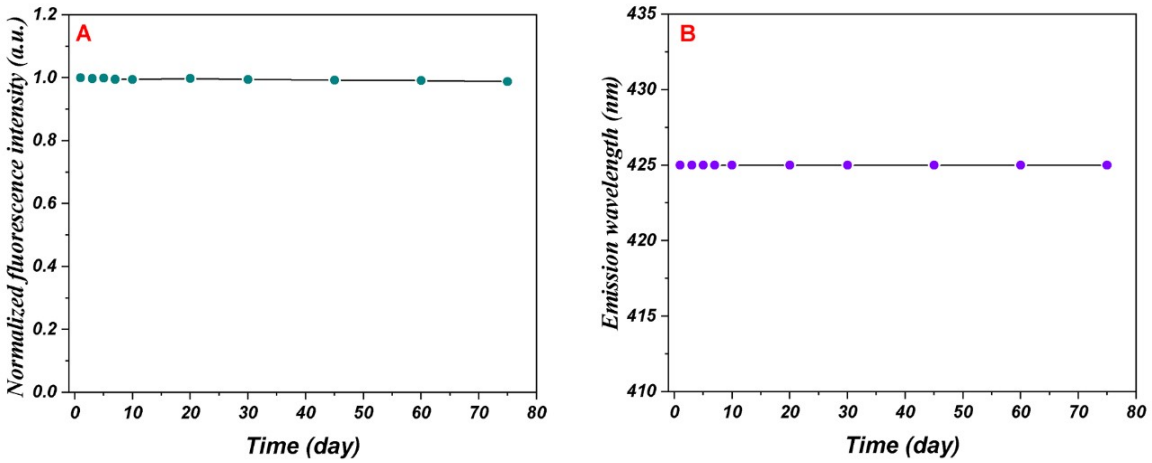

Figure S3. Stability of the as-prepared APDP-CDs with respect to (A) fluorescence emission intensity at 425 nm, and (B) emission wavelength with the maximum intensity, λ_{ex} = 370 nm, [APDP-CDs] = 0.039 mg/mL.

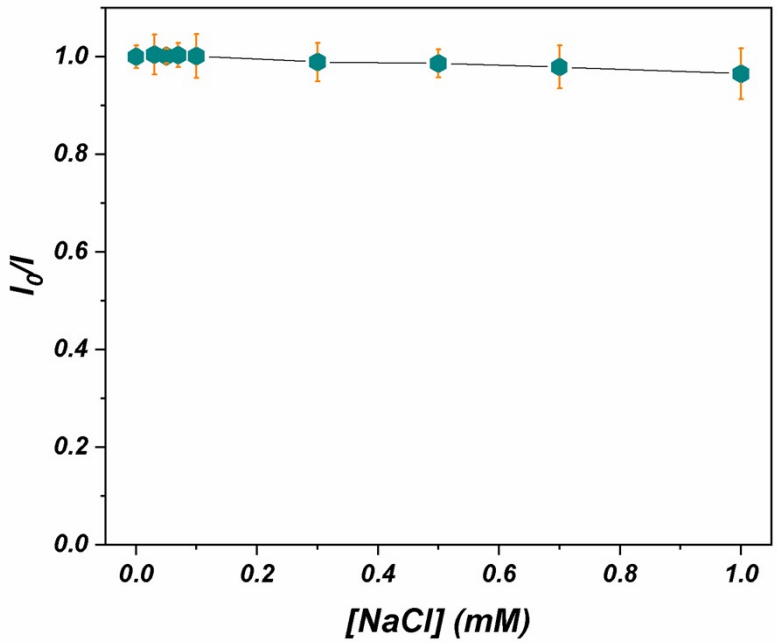

Figure S4. The relative fluorescence emission intensity of APDP-CDs in the presence of different concentrations of NaCl solutions. [APDP-CDs] = 0.039 mg/mL, λ_{ex} = 370 nm.

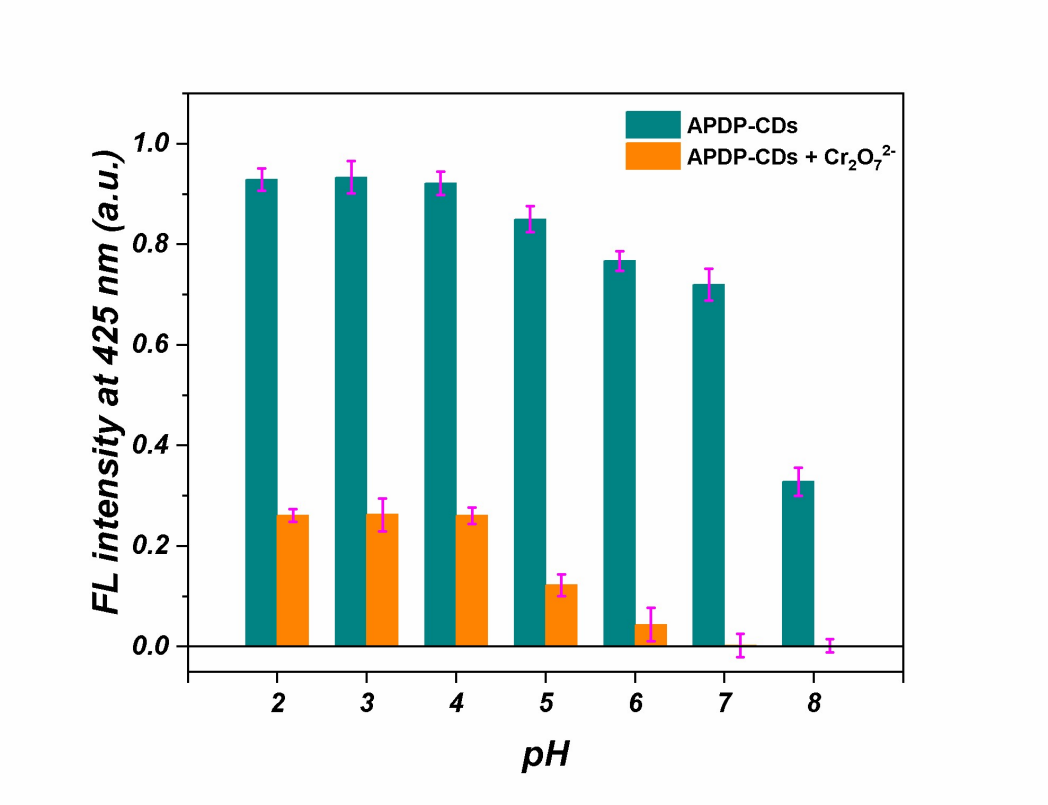

Figure S5. Bar diagram showing the influence of pH on the FL intensity at 425 nm of APDP-CDs in the absence and presence of 1 mM $Cr_2O_7^{2-}$ in various pH solutions. Determination conditions: [APDP-CDs] = 0.039 mg/mL and λ_{ex} = 370 nm.

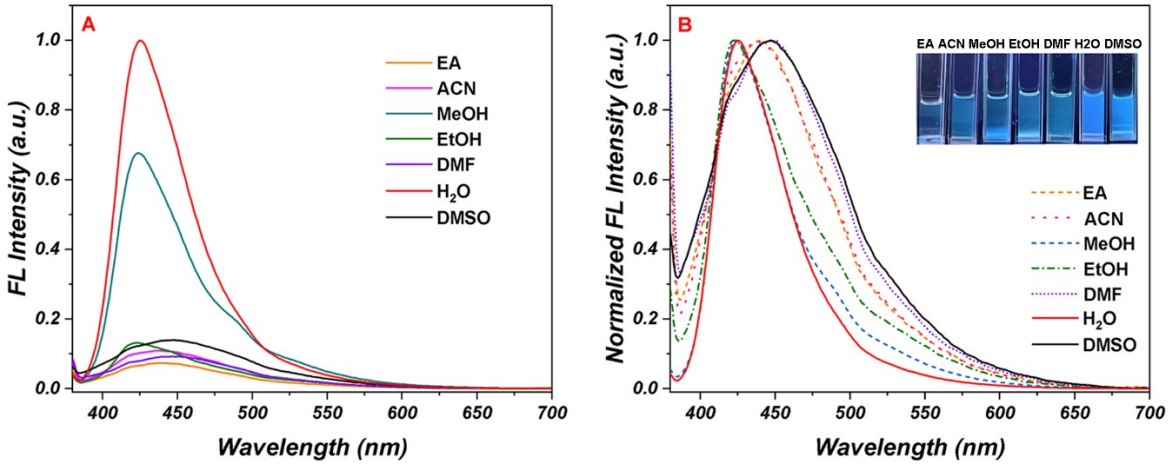

Figure S6. (A) The emission spectra and (B) normalized emission spectra of APDP-CDs in different solvents. Inset: fluorescence photos of APDP-CDs in different solvents. [APDP-CDs] = 0.039 mg/mL, λ_{ex} = 370 nm.

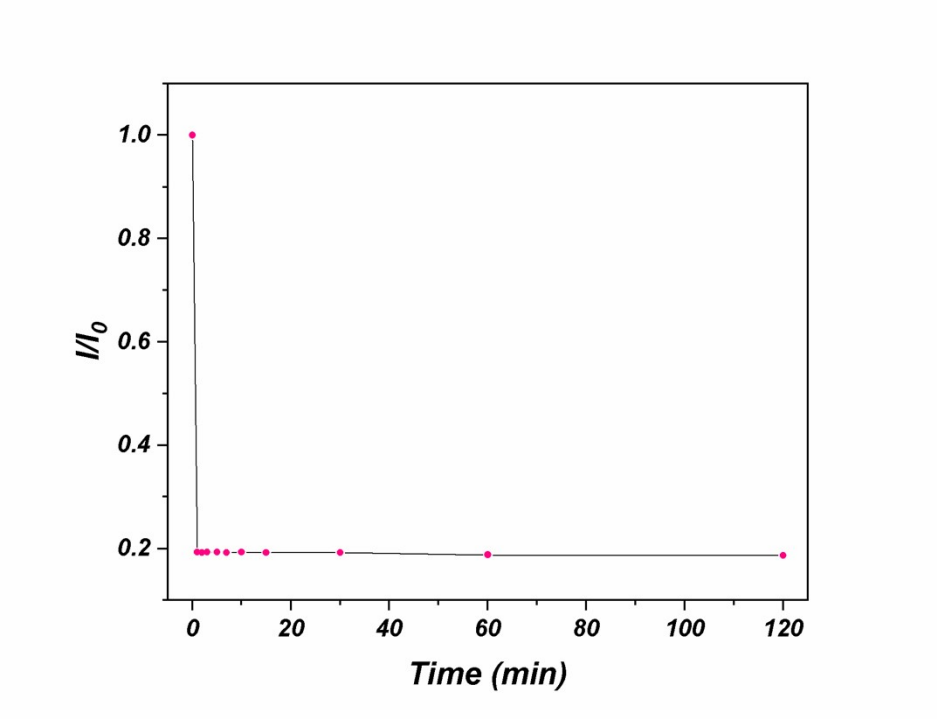

Figure S7. The relative fluorescence intensity spectra showing $Cr_2O_7^{2-}$ mediated quenching of the fluorescence of APDP-CDs with respect to time, [$Cr_2O_7^{2-}$] = 1.0 mM, [APDP-CDs] = 0.039 mg/mL, λ_{ex} = 370 nm.

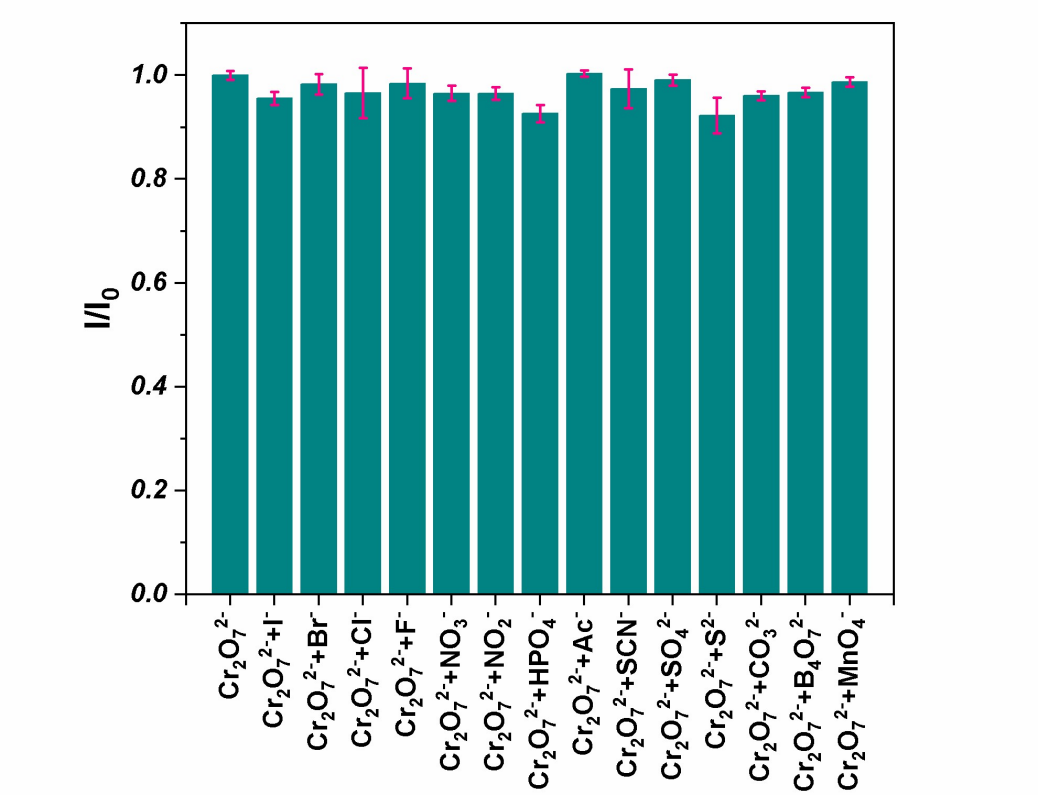

Figure S8. The relative fluorescence intensity spectra of APDP-CDs-$Cr_2O_7^{2-}$ system in the presence of various analytes, respectively. Measurement conditions: [APDP-CDs] = 0.039 mg/mL, [$Cr_2O_7^{2-}$ & interfering anions] = 100 μM, λ_{ex} = 370 nm.

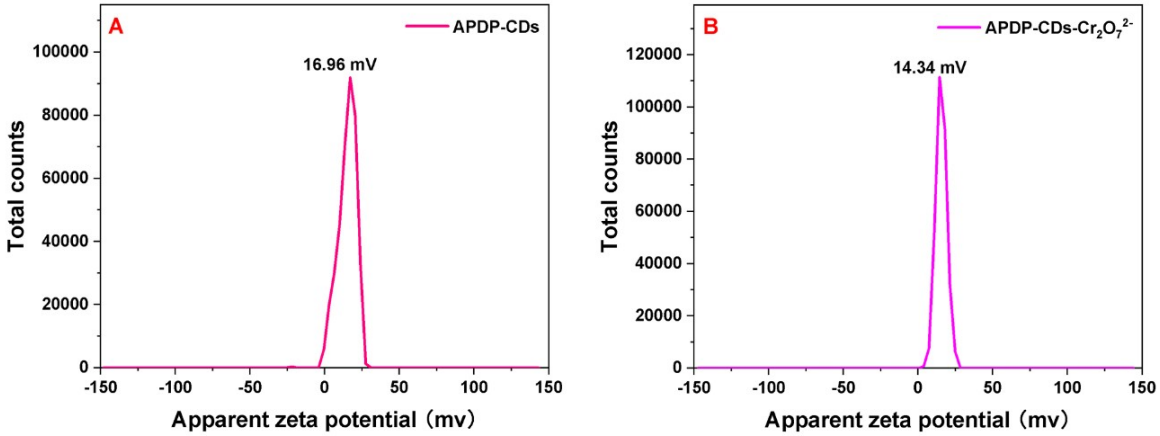

Figure S9. The zeta potential values for (A) APDP-CDs and (B) APDP-CDs-$Cr_2O_7^{2-}$ (in the presence of $Cr_2O_7^{2-}$), respectively. [APDP-CDs] = 0.039 mg/mL, [$Cr_2O_7^{2-}$] = 1 mM.

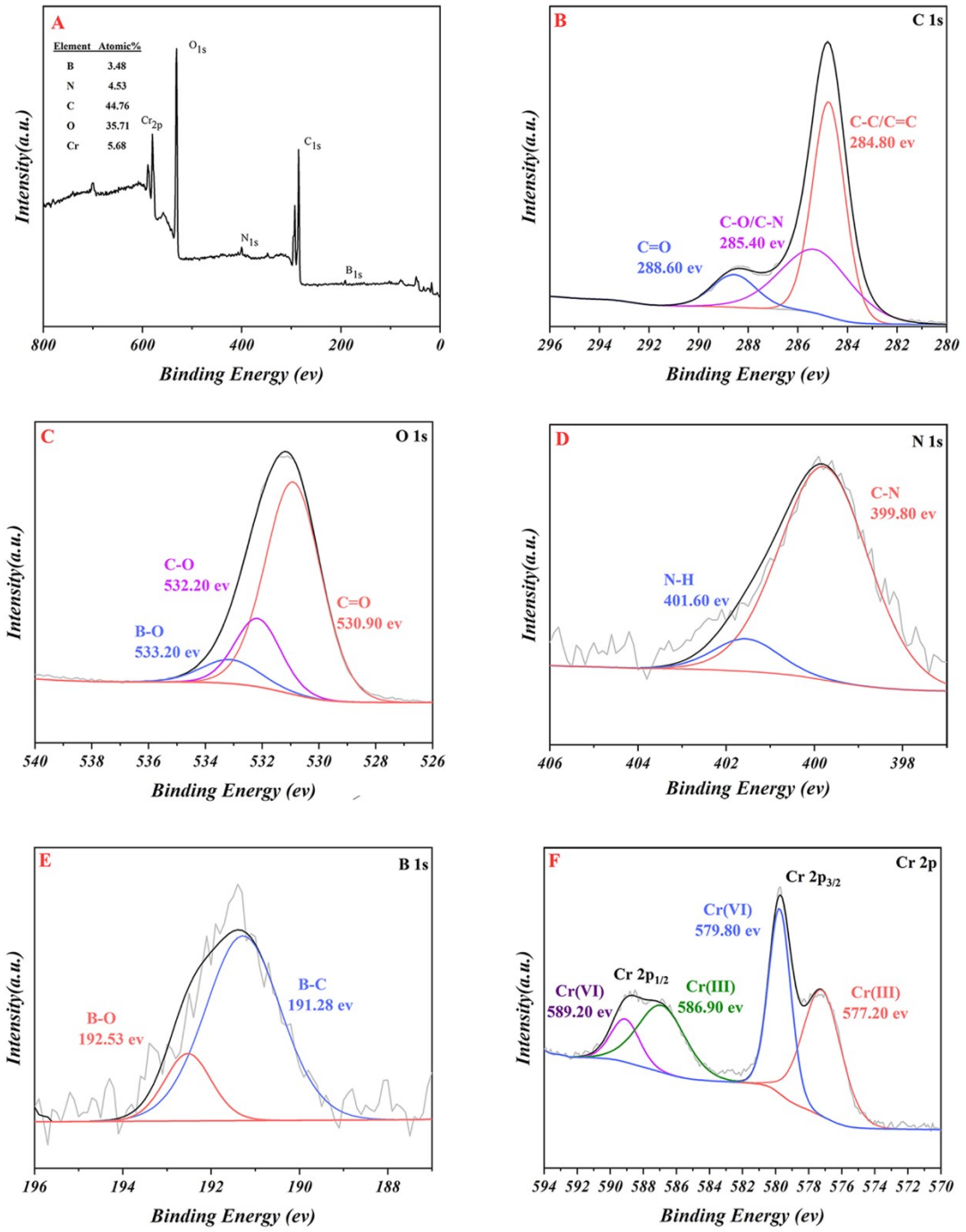

Figure S10. (A) Broad range XPS spectra of APDP-CDs-$Cr_2O_7^{2-}$. Elemental analysis of (B) C 1s, (C) O 1s, (D) N 1s, (E) B 1s and (F) Cr 2p. XPS analysis has been done using the vacuum dried solid.

Table S1. The comparison of different materials for $Cr_2O_7^{2-}$ determination.

Materials	Method of detection	Limit of detection	Linear range	QYs	Reference
N-GQDs	fluorescence	40 nM	0-140 μM	18.6%	1
CD-PEI	FAAS strategy	0.21 μg/L	–	–	2
–	chromatography	~0.5 μg/L	–	–	4
–	UA-DES-ELPME-FAAS	5.5 μg/L	–	–	6
M-Cdots	fluorescence	0.67 μM	2-100 μM	4.9%	11
CDs	fluorescence	0.14 μM	0.1-5 μM	–	12
	Colorimetric	0.41 μM	0-25 μM		
BNCDs	fluorescence	0.41 μM	0-100 μM	–	37
Ag-CDs	fluorescence	0.0437μM	0.1-0.6 μM	–	40
chemosensor	fluorescence	0.175 μM	1-500 μM	–	41
CTAB-LaHAP@PANI	adsorption	98.20 mg/g	–	–	42
Chitosan cross-linked hydrous cerium-copper oxide (CHCCO)	adsorption	297.62 mg/g	5-400 mg/L	–	43
APDP-CDs	**fluorescence**	**19 nM**	**300 nM-80 μM**	**37.6%**	**Present work**
		0.17 μM	**80 μM -1 mM**		

Table S2. The lifetime of APDP-CDs in the absence and presence of 1 mM $Cr_2O_7^{2-}$, respectively.

Moiety	τ_1 **ns**	α_1 **(%)**	τ_2 **ns**	α_2 **(%)**	τ_3 **ns**	α_3 **(%)**	τ_{av} **ns**
APDP-CDs	1.8823	1.33	4.124	95.07	17.27	3.61	5.91
APDP-CDs-$Cr_2O_7^{2-}$	0.41	0.01	3.5844	92.49	8.4965	7.5	4.38

The average lifetime (τ_{av}) has been calculated using the following equation,

$$\tau_{av} = \frac{\sum_{n=1}^{x} \alpha_n \tau_n^2}{\sum_{n=1}^{x} \alpha_n \tau_n} \quad \text{(S2)}$$

References

1. F. Cai, X. Liu, S. Liu, H. Liu and Y. Huang, *RSC Advance*, 2014, **4**, 52016-52022.

2. Y. Liu, J. Hu, Y. Li, H.-P. Wei, X.-S. Li, X.-H. Zhang, S.-M. Chen and X.-Q. Chen, *Talanta*, 2015, **134**, 16-23.

4. E. Yilmaz and M. Soylak, *Talanta*, 2016, **160**, 680-685.

6. H. Hagendorfer and W. Goessler, *Talanta*, 2008, **76**, 656-661.

11. S.-N. Zhang, L.-L. Wang, T.-T. Xiao, M. Zhang and X.-B. Yin, *Analytical and Bioanalytical Chemistry*, 2024, **416**, 3985-3996.

12. G. Qiao, D. Lu, Y. Tang, J. Gao and Q. Wang, *Dyes and Pigments*, 2019, **163**, 102-110.

27. L. Wang, J. S. Chung and S. H. Hur, *Dyes and Pigments*, 2019, **171**, 107752.

29. L. Wang, J. Jana, J. S. Chung and S. H. Hur, *Dyes and Pigments*, 2021, **186**, 109028.

37. M. Jia, L. Peng, M. Yang, H. Wei, M. Zhang and Y. Wang, *Carbon*, 2021, **182**, 42-50.

40. C. Zhao, X. Li, C. Cheng and Y. Yang, Microchemical Journal, 2019, 147, 183-190.

41. B. Hu, Y. Ma and N. Wang, Microchemical Journal, 2020, 157, 104855.

42. R. Priyadharshini, S. S. Elanchezhiyan, K. Ramkumar and S. Meenakshi, Journal of Molecular Liquids, 2024, 409, 125529.

43. A. Ghosh, S. Mondal, S. Kanrar, A. Srivastava, M. D. Pandey, U. C. Ghosh and P. Sasikumar, International Journal of Biological Macromolecules, 2024, 276, 134016.